Deployable Structures

Proceedings of the 12th Asian Pacific Conference on Shell & Spatial Structures, APCS2018
"Recent Innovations in Analysis, Design and Construction of Shell & Spatial Structures"
October 29 - 31, 2018, Penang, Malaysia
J.Y.Liew, Mustafasanie M.Y. and K.K.Choong(eds.)

Group Theoretic Approach to Detecting Finite Mechanisms of Bar-Hinge Models of Retractable Structures

Ryo WATADA[a*], Makoto OHSAKI [b], Yoshihiro KANNO [c]

*Kyoto University, Kyoto-Daigaku Katsura, Nishikyo, Kyoto 615-8540, Japan
E-mail: se.watada@archi.kyoto-u.ac.jp

[a] Takenaka Corporation
[b] Kyoto University
[c] The University of Tokyo

Abstract

A three-dimensional bar-hinge mechanism with dihedral symmetry is investigated. A group-theoretic approach is used for modeling symmetry properties. Symmetry of compatibility equations has the equivariance to the group of geometrical transformations which retain the frame configuration invariant. The number of the compatibility conditions is reduced by formulating them with respect to the null space of the linear compatibility matrix. The system of the reduced compatibility equation inherits group equivariance from the original compatibility equations. Symmetry conditions are expressed by the irreducible representation of dihedral symmetry in group theory, and sufficient conditions for finite mechanism are derived based on the symmetry conditions of mechanism modes and generalized self-equilibrium force modes. The proposed approach is examined in a numerical example with dihedral symmetry properties.

Keywords: bar-joint mechanism, arbitrarily inclined hinge, group theory, dihedral group

1. Introduction

Linkage mechanism, as shown in Figure 1, is a structure which consists of linkages connected by joints or hinges and can deform without external load. Especially, a linkage mechanism is called infinitesimal mechanism if it can have only infinitesimal deformation without external load. By contrast, a mechanism is called finite mechanism if it can have large deformation without external load. Ohsaki *et al.* [5] proposed an optimization-based approach for generating infinitesimal mechanisms which include hinges in arbitrary directions, where a quadratic programming problem is solved to obtain an infinitesimal mechanism of a frame. Guest and Fowler [1] showed that a mechanism is finite if it has no self-equilibrium force, or the self-equilibrium forces are in a different symmetry property from the deformation mode.

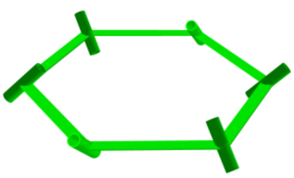

Figure 25: A hexagonal bar-hinge mechanism as an example of linkage. Six bars are connected by six revolute joints (hinges).

For modelling symmetry properties, group theory has been used in various fields. Ikeda and Murota [2] presented a group-theoretic approach to investigation of buckling behaviors of symmetric structures. Kanno *et al.* [3] investigated semidefinite programming problems whose data have group-symmetry properties.

Ikeshita [4] applied the group-theoretic bifurcation theory to the pin-jointed bar structures with symmetric configurations and derived sufficient conditions for a structure with one degree of kinematical indeterminacy and one degree of statical indeterminacy to have a finite mechanism. However, his study focuses on only pin-jointed structures.

In this paper, we consider a three-dimensional bar-hinge mechanism with dihedral symmetry. The compatibility conditions at the bar-ends are reduced by formulating them with respect to the null space of the linear compatibility matrix. Symmetry conditions are expressed using the irreducible representations of dihedral symmetry, which derives sufficient conditions for large deformation mechanism based on the symmetry conditions of infinitesimal mechanism modes and generalized self-equilibrium force modes. The conditions are verified in the numerical examples.

In our notation, we use rank(・) and ker(・) to denote the rank of a matrix and the kernel space of a matrix, respectively.

2. Group equivariance of compatibility relations

2.1. Definition of incompatibility vector

A bar-hinge mechanism is modeled using a bar element proposed by Watada and Ohsaki [6] as shown in Figure 2. We define the orthogonal reference frame of undeformed state using unit vectors as $(\boldsymbol{t}_i^1, \boldsymbol{t}_i^2, \boldsymbol{t}_i^3)$, where t_i^1 is directed from the center of bar *i* to the second end node k_{i2}. Let $\boldsymbol{r}_{i1}$ and $\boldsymbol{r}_{i2}$ denote the vectors directing from the center of bar *i* to both ends connected to nodes k_{i1} and k_{i2}, respectively; i.e., $\boldsymbol{r}_{i1} = -(L_i/2)\boldsymbol{t}_i^1$ and $\boldsymbol{r}_{i2} = (L_i/2)\boldsymbol{t}_i^1$, where L_i is the length of bar *i*.

The translation vector of node *k* and the center of bar *i* with respect to the global coordinate system (x_1, x_2, x_3) are denoted by $\boldsymbol{U}_k = (U_k^1, U_k^2, U_k^3)^\top$ and $\boldsymbol{V}_i = (V_i^1, V_i^2, V_i^3)^\top$, respectively. The rotation vector of node *k* and the center of bar *i* around global axes are denoted by $\boldsymbol{\Theta}_k = (\Theta_k^1, \Theta_k^2, \Theta_k^3)^\top$ and

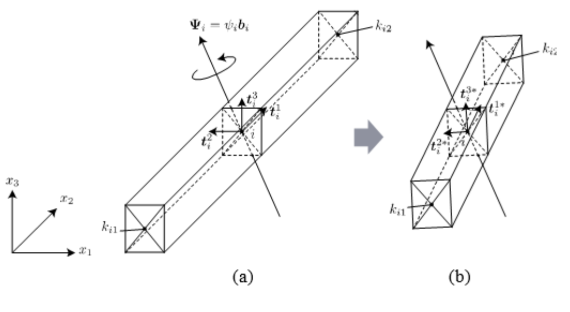

Figure 26: Definition of global coordinates, unit vectors in local coordinates, and bar rotation; (a) before deformation, (b) after deformation

$\boldsymbol{\Psi}_i = (\Psi_i^1, \Psi_i^2, \Psi_i^3)^\top$, respectively, each of which corresponds to the axis of rotation and its norm corresponds to the amount of rotation. The reference frame $(\boldsymbol{t}_i^{1*}, \boldsymbol{t}_i^{2*}, \boldsymbol{t}_i^{3*})$ in deformed state is computed from $(\boldsymbol{t}_i^1, \boldsymbol{t}_i^2, \boldsymbol{t}_i^3)$ at the undeformed state; see [6] for details.

Let $\Delta\boldsymbol{U}_{i1}, \Delta\boldsymbol{U}_{i2} \in \mathbb{R}^3$ and $\Delta\boldsymbol{\Theta}_{i1}, \Delta\boldsymbol{\Theta}_{i2} \in \mathbb{R}^3$ denote the translational and rotational incompatibility vectors, respectively, at two ends of bar *i*. If the bars are rigidly connected to nodes, the compatibility conditions are given as

$$\Delta\boldsymbol{U}_{ij} = \boldsymbol{U}_{k_{ij}} - (\boldsymbol{V}_i + \boldsymbol{r}_{ij}^*) + \boldsymbol{r}_{ij} = \boldsymbol{0}, \quad (j = 1, 2,\ i \in \mathrm{M},\ k_{ij} \in \mathrm{K}), \tag{12}$$

$$\Delta\boldsymbol{\Theta}_{ij} = \boldsymbol{\Theta}_{k_{ij}} - \boldsymbol{\Psi}_i = \boldsymbol{0}, \quad (j = 1, 2,\ i \in \mathrm{M},\ k_{ij} \in \mathrm{K}), \tag{13}$$

where K and M denote the sets of indices of all nodes and bars, respectively.

The direction vectors after rotations of nodes and bars are denoted by $\boldsymbol{f}_{ij}^n$ and $\boldsymbol{f}_{ij}^b$, respectively. The compatibility conditions are given as the collinearity of vectors $\boldsymbol{f}_{ij}^n$ and $\boldsymbol{f}_{ij}^b$, which are expressed with the independent two components of the equation expressed by the vector product as $\boldsymbol{e}_{ij} = \boldsymbol{f}_{ij}^b \times \boldsymbol{f}_{ij}^n = \boldsymbol{0}$, that is,

$$\boldsymbol{e}_{ij}^{(2)} = [e_{ij}^1, e_{ij}^2]^\top = \boldsymbol{0}. \tag{14}$$

The condition (2) is to be replaced by (3) and the number of constraints is to be reduced by one if a hinge exists at the *j*th end of bar *i*. As an assemblage of (1), (2) and (3), the compatibility equation is expressed as follows:

$$\boldsymbol{C}(\boldsymbol{W}) = \boldsymbol{0}, \tag{15}$$

where $\boldsymbol{W} \in \mathbb{R}^f$ is the *generalized displacement vector* consisting of $\boldsymbol{U}, \boldsymbol{\Theta}, \boldsymbol{V}$ and $\boldsymbol{\Psi}$, and $\boldsymbol{C}(\boldsymbol{W}) \in \mathbb{R}^m$ is called *incompatibility vector* which represents incompatibility of displacements and rotations at two ends of each bar.

2.2. Group equivariance of compatibility relations

Suppose the frame has geometrical symmetry expressed using group representation. Let *G* denote the group of geometrical transformation *g* which retain the frame configuration invariant. Then, the symmetry of compatibility equations (4) has the following *equivariance* to a group *G*.

$$S(g)\boldsymbol{C}(\boldsymbol{W}) = \boldsymbol{C}(T(g)\boldsymbol{W}), \quad g \in G, \tag{16}$$

where $S(g) \in \mathbb{R}^{m \times m}$ is a unitary matrix representation of $g \in G$ in the *m*-dimensional space expressing the transformation of incompatibility vector by action *g*, whereas $T(g) \in \mathbb{R}^{f \times f}$ is a unitary matrix representation of *g* in the *f*-dimensional space of generalized displacement vector. Equation (5) implies that if $\boldsymbol{W}$ satisfies (4), then $T(g)\boldsymbol{W}$ also satisfies $\boldsymbol{C}(T(g)\boldsymbol{W})=\boldsymbol{0}$ for any $g \in G$.

The linear compatibility matrix is denoted by $\boldsymbol{\Gamma}(\boldsymbol{W}) \in \mathbb{R}^{m \times f}$, whose (s,i) component denoted by $\Gamma_{si}(\boldsymbol{W})$ is defined as

$$\Gamma_{si}(\boldsymbol{W}) = \frac{\partial C_s(\boldsymbol{W})}{\partial W_i}. \tag{17}$$

Differentiating (6) with respect to $\boldsymbol{W}$, we have the *equivariance of the compatibility matrix* to G as follows:

$$S(g)\Gamma(\boldsymbol{W}) = \Gamma(T(g)\boldsymbol{W})T(g), \quad g \in G. \tag{18}$$

2.3. Reduction of compatibility equation

The number of compatibility equations (4) is reduced by the *Liapunov-Schmidt reduction procedure*. Let Γ_* denote the compatibility matrix at the undeformed state $\boldsymbol{W}$=**0** as $\Gamma_* = \Gamma(\boldsymbol{0})$. We define u, p and q as

$$u = \mathrm{rank}(\Gamma_*), \quad p = f - u, \quad q = m - u. \tag{19}$$

Consider a direct sum decomposition of the spaces of $\boldsymbol{W} \in \mathbb{R}^f$ and $\boldsymbol{C}(\boldsymbol{W}) \in \mathbb{R}^m$, respectively, as $\mathbb{R}^f = \ker(\Gamma_*) \oplus U$ and $\mathbb{R}^m = V \oplus \mathrm{range}(\Gamma_*)$. We take an orthonormal basis $\{\boldsymbol{\eta}_i |\, i = 1, \ldots, f\}$ of $\mathbb{R}^f$ such that $\{\boldsymbol{\eta}_i |\, i = 1, \ldots, p\}$ is a basis of $\ker(\Gamma_*)$ and $\{\boldsymbol{\eta}_i |\, i = p+1, \ldots, f\}$ is a basis of U. Similarly, we take an orthonormal basis $\{\boldsymbol{\zeta}_i |\, i = 1, \ldots, m\}$ of $\mathbb{R}^m$ such that $\{\boldsymbol{\zeta}_i |\, i = 1, \ldots, q\}$ is a basis of V and $\{\boldsymbol{\zeta}_i |\, i = q+1, \ldots, m\}$ is a basis of $\mathrm{range}(\Gamma_*)$. It should be remarked that $\boldsymbol{\eta}_1, \ldots, \boldsymbol{\eta}_p$ are *infinitesimal mechanism mode* which satisfy $\Gamma_* \boldsymbol{\eta}_i = \boldsymbol{0}$ $(i = 1, \ldots, p)$. On the other hand, because $\Gamma_*^{\top}$ is regarded as a generalized equilibrium matrix, we call $\boldsymbol{\zeta}_1, \ldots, \boldsymbol{\zeta}_q$ as *generalized self-equilibrium force mode vectors*.

The vector $\boldsymbol{W}$ is additively decomposed into two components $\boldsymbol{w} \in \ker(\Gamma_*)$ and $\overline{\boldsymbol{w}} \in U$, and $\overline{\boldsymbol{w}}$ is eliminated using the implicit function theorem. Although the details are omitted, we obtain the *reduced system of compatibility equations* with respect to $\boldsymbol{w}$ as

$$\boldsymbol{C}(\boldsymbol{w}) := P \cdot \boldsymbol{C}(\boldsymbol{w} + \phi(\boldsymbol{w})) = \boldsymbol{0}. \tag{20}$$

Let $\boldsymbol{v} := [v_1, \ldots, v_p]^{\top} \in \mathbb{R}^p$ denote a p-dimensional vector to express $\boldsymbol{w} \in \ker \Gamma_*$ using the infinitesimal mechanism modes $\{\boldsymbol{\eta}_i |\, i = 1, \ldots, p\}$ as $\boldsymbol{w} = [\boldsymbol{\eta}_1, \ldots, \boldsymbol{\eta}_p]^{\top} \boldsymbol{v}$. Then, since $\boldsymbol{C}(\boldsymbol{w})$ defined by (9) is an m-dimensional vector projected onto q-dimensional subspace V of $\mathbb{R}^m$ with respect to $\boldsymbol{w}$ expressed by $\boldsymbol{v}$, $\boldsymbol{C}(\boldsymbol{w})$ can be expressed by a q-dimensional coefficient vector $\boldsymbol{C}(\boldsymbol{v}) = [\hat{C}_1(\boldsymbol{v}), \ldots, \hat{C}_q(\boldsymbol{v})]^{\top} \in \mathbb{R}^q$ for the generalized self-equilibrium force modes $\{\boldsymbol{\zeta}_i |\, i = 1, \ldots, q\}$ as follows:

$$\boldsymbol{C}(\boldsymbol{w}) = \sum_{i=1}^{q} \hat{C}_i(\boldsymbol{v}) \boldsymbol{\zeta}_i = [\boldsymbol{\zeta}_1, \ldots, \boldsymbol{\zeta}_q] \boldsymbol{C}(\boldsymbol{v}). \tag{21}$$

2.4. Group equivariance of reduced compatibility equation

The reduction procedure described above is applied to the system of compatibility equations which has group equivariance shown in (5). It can be shown that the system of reduced compatibility equation (9) inherits group equivariance (5) from the original compatibility equation (4). That is, group equivariance of the reduced compatibility (9) is expressed as

$$S(g)\boldsymbol{C}(\boldsymbol{w}) = \boldsymbol{C}(T(g)\boldsymbol{w}), \quad g \in G. \tag{22}$$

Equation (10) reduces the group equivariance (11) to

$$S(g)\boldsymbol{C}(\boldsymbol{v}) = \boldsymbol{C}(T(g)\boldsymbol{v}), \quad g \in G, \tag{23}$$

where $\hat{S}(g) \in \mathbb{R}^{q\times q}$ and $\hat{T}(g) \in \mathbb{R}^{p\times p}$ satisfy the following equations:

$$S(g)[\boldsymbol{\zeta}_1,\ldots,\boldsymbol{\zeta}_q] = [\boldsymbol{\zeta}_1,\ldots,\boldsymbol{\zeta}_q]S(g), \quad g \in G, \tag{24}$$

$$T(g)[\boldsymbol{\eta}_1,\ldots,\boldsymbol{\eta}_p] = [\boldsymbol{\eta}_1,\ldots,\boldsymbol{\eta}_p]\hat{T}(g), \quad g \in G. \tag{25}$$

See Watada *et al.* [7] for details.

3. Prediction of large-deformation property of D$_n$-equivariant system

From this section, we focus on frames which have dihedral symmetry and show a method to investigate whether the frame has finite mechanism or not using the reduced group equivariance (12).

Dihedral symmetry of *n*th order, expressed by D_n, is symmetry properties of a regular *n*-sided polygon, which includes *n* degrees of rotational symmetry and *n* axes of reflection symmetry. Figure. 3 shows a example of D_n where *n* is 3. Dihedral group D_n is written as

$$\mathrm{D}_n = \left\{e, r, \ldots, r^{n-1}, s, sr, \ldots, sr^{n-1}\right\}, \tag{26}$$

where *r* , *s* and *e* denote a counterclockwise rotation around *z*-axis by an angle $2\pi/n$, a reflection with respect to *xz* plane and the identity transformation, respectively, as shown in Figure 3. Note that *r* and *s* have the relations $r^i r^j = r^{i+j}$ and $r^n = s^2 = (sr)^2 = e$.

In this study, we consider the case where a D_n symmetric frame has a single infinitesimal mechanism mode and a single generalized mechanism mode, i.e., G=D_n, $p = f - u = 1$ and $q = m - u = 1$. Hereinafter, we define ξ as a *path parameter* defining deformation of the frame as follows:

$$\xi := v_1 \in \mathbb{R}. \tag{27}$$

Then, (12) is rewritten as following equation:

$$S(g)C(\xi) = C(T(g)\xi), \quad g \in G. \tag{28}$$

Since $\hat{T}(g)$ and $\hat{S}(g)$ are 1×1 matrix representations of *G*, they are irreducible. Then, let ν and μ denote the irreducible representation indices of these matrix representations, respectively.

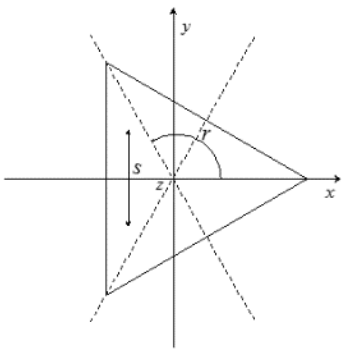

Figure 27: Dihedral symmetry of 3rd order D_3.

We remark that ν and its one-dimensional representations $T^{\nu}(g)(=\hat{T}(g))$ are expressed as follows:

$$\nu \in \begin{cases} \{A_1, A_2, B_1, B_2\} & \text{(for } n \text{ even)} \\ \{A_1, A_2\} & \text{(for } n \text{ odd)} \end{cases}, \tag{29}$$

where

$$T^{A_1}(r)=1, \quad T^{A_1}(s)=1, \tag{30a}$$

$$T^{A_2}(r)=1, \quad T^{A_2}(s)=-1, \tag{19b}$$

$$T^{B_1}(r)=-1, \quad T^{B_1}(s)=1, \tag{19c}$$

$$T^{B_2}(r)=-1, \quad T^{B_2}(s)=-1. \tag{19d}$$

We can judge which of (19a)-(19d) is satisfied from the property of rotational and reflectional symmetry of infinitesimal mechanism mode $\boldsymbol{\eta}_1$, or by simply calculating from $T(g)$ and $\boldsymbol{\eta}_1$ as $T^{\nu}(r)=\boldsymbol{\eta}_1^{\cdot} T(r)\boldsymbol{\eta}_1$ and $T^{\nu}(s)=\boldsymbol{\eta}_1^{\cdot} T(s)\boldsymbol{\eta}_1$.

Similarly, μ and $S^{\mu}(g)(=\hat{S}(g))$ are determined from

$$\mu \in \begin{cases} \{A_1, A_2, B_1, B_2\} & \text{(for } n \text{ even)} \\ \{A_1, A_2\} & \text{(for } n \text{ odd)} \end{cases}, \tag{31}$$

and

$$S^{A_1}(r)=1, \quad S^{A_1}(s)=1, \tag{32a}$$

$$S^{A_2}(r)=1, \quad S^{A_2}(s)=-1, \tag{21b}$$

$$S^{B_1}(r)=-1, \quad S^{B_1}(s)=1, \tag{21c}$$

$$S^{B_2}(r)=-1, \quad S^{B_2}(s)=-1. \tag{21d}$$

where μ is determined from the symmetry property of generalized self-equilibrium force mode $\boldsymbol{\zeta}_1$, or from (21a)-(21d) and calculation of $S^{\mu}(r)=\boldsymbol{\zeta}_1^{\cdot} S(r)\boldsymbol{\zeta}_1$ and $S^{\mu}(s)=\boldsymbol{\zeta}_1^{\cdot} S(s)\boldsymbol{\zeta}_1$.

Equation (17) is finally rewritten as

$$S^{\mu}(g)C(\xi)=C(T^{\nu}(g)\xi), \quad g \in G. \tag{33}$$

From (22), combinations of ν and μ representing sufficient conditions for existence of a finite mechanism are derived. For example, consider the case that ν and μ are determined as $\nu = A_1$ and $\mu = A_2$. In this case, there exists an element $h=s$ of G satisfying $T^{\nu}(h)=1$ and $S^{\mu}(h)=-1$. Then, substituting $g=h$ to (22), we obtain following relation:

$$-C(\xi)=C(\xi) \quad \Leftrightarrow \quad C(\xi)=0. \tag{34}$$

This means that the reduced incompatibility $\hat{C}(\xi)$ remains 0 identically for any path parameter ξ of deformation; that is, the frame has a finite mechanism.

Table 1: Combination of ν and μ for existence of a finite mechanism

		μ			
		A_1	A_2	B_1	B_2
ν	A_1	unknown	o	o	o
	A_2	even	odd	o	o
	B_1	even	o	odd	o
	B_2	even	o	o	odd

In the similar manner, combinations of ν and μ so that the frame has a finite mechanism is summarized in Table 1 with letter 'o'. In Table 1, 'even' and 'odd' indicate that the corresponding $\hat{C}(\xi)$ are an even function and an odd function, respectively.

4. Numerical Examples

For a numerical example, we consider 6-bar linkage in *xy*-plane as shown in Figure 4(a). Also, Figure 4(b) represents a physical model of this linkage. The number of members m_0 is 6 and the number of nodes n_0 is 6. In Figure 4(a), the numbers in ( ) and < > express indices of bars and nodes, respectively. Each bar has hinges at both ends as shown in Figure 4(a) with dashed lines, and any two hinges connected to the same node are parallel. Note that the hinges are assigned duplicately to clearly investigate the symmetry property. A pair of hinges at the same node is combined to a single hinge, when making a physical model as shown in Figure 4(b). In Figure 4(a), all lines of the axes of hinges at nodes 1, 3 and 5 intersect with *z*-axis at (0, 0, $-\tan\alpha_1$), and all lines of the axes of hinges at nodes 2, 4 and 6 intersect with *z*-axis at (0, 0, $-\tan\alpha_0$). Then, the direction vector $f_{k_{ij}}$ of hinge axis between *j*th end of bar *i* and node k_{ij} is expressed as follows:

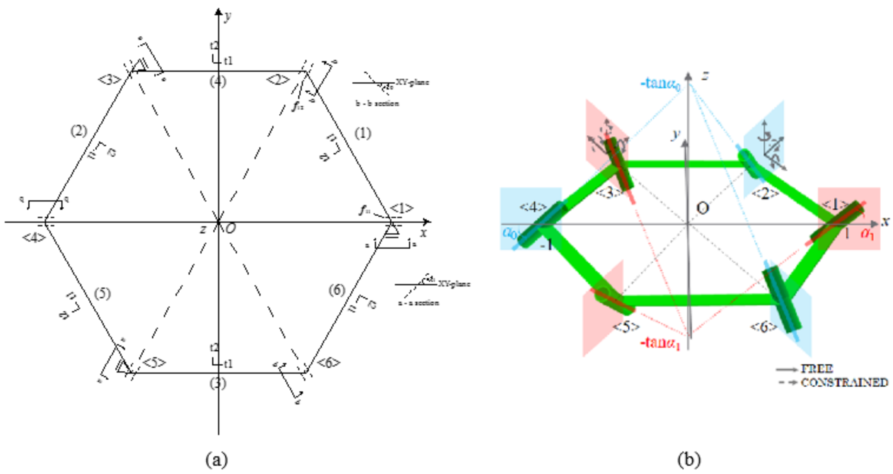

Figure 28: 6-bar linkage; (a) bar-hinge mechanism model, (b) physical model with constraints and hinge-directions

$$\boldsymbol{f}_{k_{ij}} = \left[\cos\alpha_1 \cos\frac{(k_{ij}-1)\pi}{3}, \cos\alpha_1 \sin\frac{(k_{ij}-1)\pi}{3}, \sin\alpha_1 \right]^{\top}, \quad \text{for } k_{ij} = 1,3,5\,, \tag{35}$$

$$\boldsymbol{f}_{k_{ij}} = \left[\cos\alpha_0 \cos\frac{(k_{ij}-1)\pi}{3}, \cos\alpha_0 \sin\frac{(k_{ij}-1)\pi}{3}, \sin\alpha_0 \right]^{\top}, \quad \text{for } k_{ij} = 2,4,6\,. \tag{36}$$

The origin of coordinate axes is denoted by *O* in Figure 4(a) and 4(b). Let l_k^1, l_k^2, l_k^3 denote the unit vectors of local coordinate at node *k*, where l_k^1 is the unit vector directed from *O* to node *k* and l_k^2 and l_k^3 satisfy $\boldsymbol{l}_k^2 = [0,0,1]^{\top} \times \boldsymbol{l}_k^1$ and $\boldsymbol{l}_k^3 = \boldsymbol{l}_k^1 \times \boldsymbol{l}_k^2$, respectively. To prevent the indefiniteness of rotation angles around the axes of two hinges connected to the same node, we add the compatibility equations with respect to $\boldsymbol{\Theta}_k\ (k = 1,\ldots,6)$ as follows:

$$\boldsymbol{l}_k^{1\top} \boldsymbol{\Theta}_k = 0, \quad \text{for k} = 1,\ldots,6\,. \tag{37}$$

Moreover, we consider the constraints that translations $\boldsymbol{U}_k$ at node 1, 3 and 5 are allowed only along the diagonal directions passing through the origin *O* as

$$\boldsymbol{l}_k^{2\top} \boldsymbol{U}_k = 0, \quad \text{for k} = 1,3,5\,, \tag{38}$$

$$\boldsymbol{l}_k^{3\top} \boldsymbol{U}_k = 0, \quad \text{for k} = 1,3,5\,. \tag{39}$$

Support constraints of translations and rotations described above are shown in Figure 4(b) with dashed arrows for nodes 2 and 3 on behalf of all nodes. As an assemblage of (26)-(28), the number of constraints *c* is 12. Considering the number of hinges *h* is 12, we have $\boldsymbol{W} \in \mathbb{R}^f$ and $\boldsymbol{C}(\boldsymbol{W}) \in \mathbb{R}^m$ as $f = 6n_0 + 6m_0$ =72 and $m = 12m_0 + c - h$ =72, respectively. Note that the support conditions are added to the compatibility conditions in this model.

From conditions of the hinges and the support constraints, it is determined that the symmetry of this model is D_3. Then, representation matrix $T(g)$ of this model is obtained by considering that $T(r)$ and $T(s)$ express the transformation of generalized displacement vector $\boldsymbol{W}$ by action *r*, a counter-clockwise rotation around *z*-axis by an angle $2\pi/3$, and action *s*, a reflection with respect to *xz* plane, respectively. Representation matrix $S(g)$ expressing the transformation of incompatibility vector $\boldsymbol{C}(\boldsymbol{W})$ is also determined in the same manner.

Let $\alpha_1 = \pi/4$ and $\alpha_0 = -\pi/4$. From the Singular Value Decomposition (SVD) of Γ_*, $u = \mathrm{rank}(\Gamma_*)$ is obtained as 71. Additionally, one infinitesimal mechanism mode $\boldsymbol{\eta}_1$ and one generalized self-equilibrium force mode $\boldsymbol{\zeta}_1$ are also obtained from SVD because $p = f - u = 1$ and $q = m - u = 1$. Figures 5(a) and 5(b) show obtained infinitesimal mechanism $\boldsymbol{\eta}_1$ and generalized self-equilibrium force mode $\boldsymbol{\zeta}_1$, respectively. Note that irreducible representation index of $\boldsymbol{\eta}_1$ is $\nu = A_1$, because we confirmed that $T^{\nu}(r) = \boldsymbol{\eta}_1^{\top} T(r)\boldsymbol{\eta}_1 = 1$ and $T^{\nu}(s) = \boldsymbol{\eta}_1^{\top} T(s)\boldsymbol{\eta}_1 = 1$. Similarly, irreducible representation index of $\boldsymbol{\zeta}_1$ is $\mu = A_2$, because $S^{\mu}(r) = \boldsymbol{\zeta}_1^{\top} S(r)\boldsymbol{\zeta}_1 = 1$ and $S^{\mu}(s) = \boldsymbol{\zeta}_1^{\top} S(s)\boldsymbol{\zeta}_1 = -1$. These indices of $\boldsymbol{\eta}_1$ and $\boldsymbol{\zeta}_1$ can also be determined by whether these modes are symmetric or anti-symmetric with respect to action *r* and *s*, respectively.

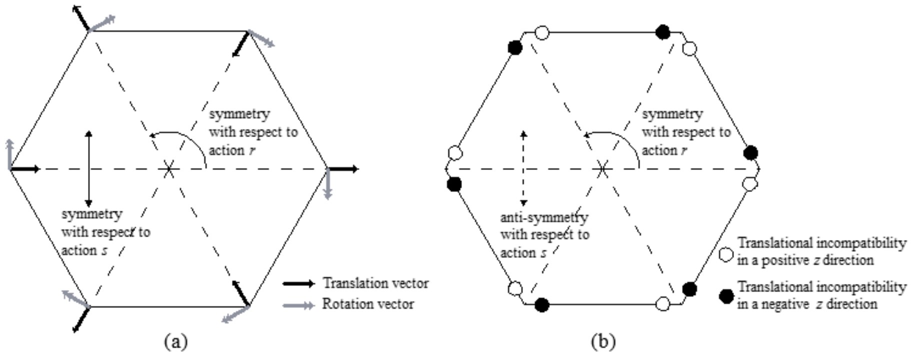

Figure 29: Infinitesimal mechanism mode and generalized self-equilibrium force mode of the 6-bar linkage; (a) Infinitesimal displacement mode η_1, (b) Generalized self-equilibrium force mode ζ_1

Finally, this combination of (ν, μ) is included in Table 1 with letter 'o', which means this linkage has one finite mechanism.

5. Conclusion

Properties of a three-dimensional bar-hinge mechanism with dihedral symmetry has been investigated. A group-theoretical approach is applied to derive sufficient conditions for existence of finite mechanism of the bar-hinge mechanism which has single infinitesimal mechanism mode and single generalized self-equilibrium force mode. The results have been confirmed in the numerical example of a 6-bar linkage.

References

[1] Guest SD. and Fowler PW., Symmetry conditions and finite mechanisms. J. Mech. Mater. Struct., 2007; 2(2); 293-301.

[2] Ikeda K. and Murota K., Imperfect Bifurcation in Structures and Materials (2nd ed.), Applied Mathematical Sciences, Springer, 2010.

[3] Kanno Y., Ohsaki M., Murota K. and Katoh N., Group symmetry in interior-point methods for semidefinite program, Optim. Eng., 2001, 2, 293-320.

[4] Ikeshita R., Bifurcation Analysis of Symmetric Mechanisms by using Group Theory (in Japanese). Graduation thesis, Department of Mathematical Engineering and Information Physics, School of Engineering, The University of Tokyo, 2013.

[5] Ohsaki M., Tsuda S. and Miyazu Y., Design of linkage mechanisms of partially rigid frames using limit analysis with quadratic yields functions, Int. J. Solids and Struct., 2016; 88-89; 68-78.

[6] Watada R. and Ohsaki M., Series expansion method for determination of order of 3-dimensional bar-joint mechanism with arbitrarily inclined hinges, Int. J. Solids and Struct., 2018; published online, doi: 10.1016/j/ijsolstr.2018.02.012.

[7] Watada R., Ohsaki M. and Kanno Y., Group theoretic approach to large-deformation property of three-dimensional bar-hinge mechanism, Japan Journal of Industrial and Applied Mathematics, under review.